

# CALCULATION OF 3D TURBULENT JETS IN CROSSFLOW WITH A MULTIGRID METHOD AND A SECOND-MOMENT CLOSURE MODEL

A.O. Demuren\*  
Institute for Computational Mechanics in Propulsion  
Lewis Research Center  
Cleveland, Ohio 44135

## ABSTRACT

A multigrid method is presented for calculating turbulent jets in crossflow. Fairly rapid convergence is obtained with the  $k - \epsilon$  turbulence model, but computations with a full Reynolds stress turbulence model (RSM) are not yet very efficient. Grid dependency tests show that there are slight differences between results obtained on the two finest grid levels. Computations using the RSM are significantly different from those with  $k - \epsilon$  model and compare better to experimental data. Some work is still required to improve the efficiency of the computations with the RSM.

---

\*Work Funded under Space Act Agreement C99066G.

## NOMENCLATURE

---

$c_1, c_s$	constant in Reynolds stress model
$c_\mu, c_{\epsilon 1}, c_{\epsilon 2}$	$k - \epsilon$ turbulence model constants
D	jet diameter
f	near-wall proximity function in Reynolds stress model
G	rate of production of turbulent kinetic energy
H	height of duct
k	turbulent kinetic energy
P	pressure
R	jet to crossflow velocity ratio
S	pitch spacing of multiple jets
$S_\phi$	source term for dependent variable $\Phi$
$U_\infty$	crossflow velocity
$U_i$	cartesian velocity components
$\overline{u_1^2}, \overline{u_2^2}, \overline{u_3^2}$	Reynolds normal stresses in cartesian directions
$\overline{u_1 u_2}, \overline{u_1 u_3}, \overline{u_2 u_3}$	Reynolds shear stresses
$V_j$	jet velocity
W	width of duct
$y^j$	cartesian coordinates
$\alpha, \beta, \gamma$	constants in Reynolds stress model
$\delta_{ij}$	Kronecker delta
$\epsilon$	rate of dissipation of turbulent kinetic energy
$\kappa$	von Karman constant
$\lambda$	thermal/species diffusivity
$\mu$	molecular viscosity
$\mu_t$	turbulent eddy viscosity
$\rho$	density
$\sigma_\phi$	turbulent Prandtl/Schmidt number for $\Phi$
$\Phi$	General representation of dependent variable

### Superscripts

1	lateral direction
2	vertical direction
3	longitudinal direction

---

## INTRODUCTION

Three-dimensional turbulent jets in crossflow have important engineering applications in both confined and unconfined environments. Examples of jets issuing into confined crossflow include internal cooling of turbine blades, dilution air jets in combustion chambers, jets from V/STOL aircraft in transition flight, etc. The examples of turbulent jets issuing into unconfined (semi-infinite) crossflow are even more numerous. These include discharges from cooling towers or chimney stacks into the atmosphere or sewerage and waste heat into water bodies, film-cooling of turbine blades, etc.

The interaction of the jets with the crossflow has been investigated in numerous experimental studies [1–4]. Crabb et al [2] present a comprehensive review of pre 1980 studies, most of which only deal with mean flow properties. Measurements of turbulent properties can be found in [2–6]. Numerous computational studies of the generic problem of turbulent jets in crossflow are also reported in the literature [7–10], but there are uncertainties as to the accuracy of the results. First, it has not been possible to obtain grid independent solutions. In a recent study, Claus and Vanka [11] present results with computational grids up to 96x96x256, but could still not confirm grid independency. Secondly, most computations have employed the  $k - \epsilon$  turbulence model which assumes gradient diffusion relations for the Reynolds stresses and an isotropic eddy-viscosity distribution. Measurements of Reynolds stresses and velocity fields by Andreopoulos and Rodi [4] suggest that these assumptions may not be appropriate in many cases.

The present study tries to address these problems. Computations are performed with a multi-grid procedure which enables convergence on very fine grids within a relatively small number of iterations. A second-moment closure turbulence model is utilised to compute the Reynolds stresses, as well as the more popular  $k - \epsilon$  model.

## MATHEMATICAL MODEL

In the present work we solve the time-averaged, three-dimensional, steady state equations governing the turbulent flow and heat transfer. The equations may be expressed in cartesian tensor notation as:

Continuity

$$\frac{\partial}{\partial y^i}(\rho U_i) = 0 \quad (1)$$

Momentum

$$\frac{\partial}{\partial y^j}(\rho U_j U_i) = -\frac{\partial}{\partial y^i} P + \frac{\partial}{\partial y^j} \left[ -\rho \overline{u_i u_j} + \mu \left( \frac{\partial U_i}{\partial y^j} + \frac{\partial U_j}{\partial y^i} \right) \right] \quad (2)$$

Temperature/Concentration

$$\frac{\partial}{\partial y^j}(\rho U_j \Phi) = S_\phi + \frac{\partial}{\partial y^j} \left[ -\rho \overline{u_i \phi} + \lambda \left( \frac{\partial \Phi}{\partial y^j} \right) \right] \quad (3)$$

with  $i=1,2,3$  and  $j=1,2,3$  representing properties in the lateral, vertical and longitudinal directions, respectively.  $y^j$  ( $= y^1, y^2, y^3$ ) represents the cartesian coordinates;  $U_i$  the cartesian velocity components;  $P$  the pressure and  $\Phi$  the normalised temperature or concentration.  $\rho$  is the density,  $\mu$  is the molecular viscosity and  $\lambda$  is the thermal or species diffusivity. The equations are expanded by using Einstein's summation rule for repeated indices.  $-\rho\overline{u_i u_j}$  and  $-\rho\overline{u_i \phi}$  are respectively, the Reynolds stresses and heat/concentration fluxes which must be determined by a turbulence model before the system of equations can be closed.

### Turbulence Model

In this paper results are presented of calculations with both the standard  $k - \epsilon$  turbulence model [12] and a second-moment turbulence closure based on the proposals of Launder, Reece and Rodi [13], hereafter denoted LRR.

In the standard  $k - \epsilon$  model, the Reynolds stresses and heat fluxes are approximated with the Boussinesq eddy viscosity/diffusivity concept as

$$-\rho\overline{u_i u_j} = \mu_t \left( \frac{\partial U_i}{\partial y^j} + \frac{\partial U_j}{\partial y^i} \right) - \frac{2}{3} k \delta_{ij} \quad (4)$$

$$-\rho\overline{u_i \phi} = \frac{\mu_t}{\sigma_\phi} \frac{\partial \Phi}{\partial y^i} \quad (5)$$

$\mu_t$  is the eddy viscosity given by :

$$\mu_t = c_\mu \rho \frac{k^2}{\epsilon} \quad (6)$$

The distributions of the turbulent kinetic energy  $k$  and its rate of dissipation  $\epsilon$  are then obtained from the solution of the transport equations:

$$\frac{\partial}{\partial y^j} (\rho U_j k) = \frac{\partial}{\partial y^j} \left( \frac{\mu_t}{\sigma_k} \frac{\partial k}{\partial y^j} \right) + G - \rho \epsilon \quad (7)$$

$$\frac{\partial}{\partial y^j} (\rho U_j \epsilon) = \frac{\partial}{\partial y^j} \left( \frac{\mu_t}{\sigma_\epsilon} \frac{\partial \epsilon}{\partial y^j} \right) + c_{\epsilon 1} G \frac{\epsilon}{k} - c_{\epsilon 2} \rho \frac{\epsilon^2}{k} \quad (8)$$

where  $G$  is the turbulence production rate given by:

$$G = -\rho\overline{u_i u_j} \frac{\partial U_i}{\partial y^j} \quad (9)$$

The empirical constants appearing in the equations above are:

$$c_\mu = 0.09, c_{\epsilon 1} = 1.44, c_{\epsilon 2} = 1.92, \sigma_t = 0.9, \sigma_k = 1.0, \sigma_\epsilon = 1.3 \quad (10)$$

and  $\delta_{ij}$  is the Kronecker delta. Equations (1)–(9) form a closed set which is solved iteratively in a sequential manner to obtain the velocity and temperature fields.

For the second-moment closure model, we adopt the proposals of LRR [13], model 1 to approximate the pressure-strain, diffusion, and dissipation terms in the Reynolds stress equations. The resulting system of equations can be written in cartesian tensor notation as:

$$\begin{aligned} \frac{\partial}{\partial y^j} (\rho U_j \overline{u_i u_j}) &= \frac{\partial}{\partial y^m} (c_s \rho \frac{k}{\epsilon} \overline{u_m u_k} \frac{\partial \overline{u_i u_j}}{\partial y^k}) - \rho \{ (1 - \alpha) [\overline{u_i u_i} \frac{\partial U_l}{\partial y^j} + \overline{u_j u_i} \frac{\partial U_l}{\partial y^i}] \\ - \beta [\overline{u_i u_i} \frac{\partial U_j}{\partial y^i} + \overline{u_j u_i} \frac{\partial U_i}{\partial y^j}] + \frac{2}{3} \delta_{ij} (\alpha + \beta) \overline{u_k u_i} \frac{\partial U_l}{\partial y^k} + \gamma k (\frac{\partial U_j}{\partial y^i} + \frac{\partial U_i}{\partial y^j}) + \frac{c_1 \epsilon}{k} (\overline{u_i u_j} - \frac{2}{3} \delta_{ij} k) + \frac{2}{3} \delta_{ij} \epsilon \} \end{aligned} \quad (11)$$

with the empirical coefficients  $\alpha, \beta, \gamma, c_1$ , and  $c_s$  given by:

$$\alpha = 0.7636 - 0.06 f; \beta = 0.1091 + 0.06 f; \gamma = 0.182; c_1 = 1.5 - 0.50 f; c_s = 0.22 \quad (12)$$

and  $f$  is the wall-proximity function with value of unity near walls and zero in a completely free stream.

To be consistent with the second-moment closure, we modify Eq. (8) slightly by introducing non-isotropic eddy-viscosity distributions into the diffusion terms, following LRR. We do not apply a second-moment closure model to the turbulent heat flux  $\overline{u_i \varphi}$  in the present study. Equations (1), (2), (3), (8) and (11) form a closed set which should be solved simultaneously. The equations are solved in a sequential manner, first for the velocity components and pressure, then Reynolds stresses and dissipation, and finally the temperature. If the terms involving gradients of the Reynolds stresses on the r.h.s. of Eq. (2) are treated explicitly the system of equations will be very stiff and it will be extremely difficult to obtain a converged solution with an iterative scheme. The stiffness can be reduced considerably by splitting the Reynolds stress  $\overline{u_i u_j}$  into two parts:

$$\overline{u_i u_j} = \overline{u_i u_j'} - \frac{\mu_t}{\rho} \left( \frac{\partial U_i}{\partial y^j} + \frac{\partial U_j}{\partial y^i} \right) \quad (13)$$

The first part is treated explicitly. The second part is added to the molecular diffusion term and treated implicitly. The modified momentum equation has the form:

$$\frac{\partial}{\partial y^j} (\rho U_j U_i) = - \frac{\partial}{\partial y^i} P + \frac{\partial}{\partial y^j} \left[ - \rho \overline{u_i u_j'} + (\mu + \mu_t) \left( \frac{\partial U_i}{\partial y^j} + \frac{\partial U_j}{\partial y^i} \right) \right] \quad (14)$$

The set of Eqs. (1), (3), (8) (11) and (14) is solved, using underrelaxation factors of 0.75 for the three velocity components, 0.25 for the pressure, and 0.7 for the temperature and all turbulence quantities. Four types of boundary conditions are encountered, namely: inlet, outlet, symmetry and walls. Inlet conditions are specified from experimental data. The outlet is an outflow boundary requiring no formal specification of conditions. Along symmetry planes the normal gradients of all variables are set to zero, and the normal velocity component is also zero. The walls are special in that we do not integrate all the way down, rather we use the wall-function method [12,13] to prescribe the values of the dependent variables at near-wall nodes.

### Multigrid Procedure

In the present work the FAS-FMG (full approximation storage-full multigrid) algorithm originally developed by Brandt [14] is employed to solve the hydrodynamic equations. The present implementation derives from previous works by Demuren [15] and Vanka [16]. There are however significant differences. First, the present method uses a regular grid system with no staggering of the velocity nodes relative to the pressure nodes. The expected odd-even decoupling problem is overcome by adding a fourth-order artificial dissipation term to the pressure gradient. It can be shown that, with a coefficient of unity, this practice is equivalent to the so-called "momentum interpolation" method of Peric [17]. However, there is now the flexibility to vary the coefficient all the way down to zero, if necessary. The second difference is that the system of equations is now solved in a sequential manner as opposed to the coupled approach proposed by Vanka. Numerical experiments showed no advantage in using the latter in a multigrid procedure, and it can be shown mathematically that it is less stable in a single-grid procedure. Further, it appears easier to vectorize the decoupled procedure.

The smoothing scheme is based on the SIMPLEC method described by van Doormaal and Raithby [18]. The salient steps are:

1. Solve the  $U_1$  momentum equation using a guessed pressure field.
2. Then the  $U_2$  momentum equation.
3. Then the  $U_3$  momentum equation.
4. Compute the velocities on the faces of the control volume, each by linear interpolation plus a fourth-order artificial dissipation term.
5. Then compute the mass source error in each control volume.
6. Solve a pressure-correction equation to eliminate the mass source errors, and then correct the pressures and corresponding velocity components.

7. If on the finest grid level, solve the equations for  $k$ ,  $\epsilon$ , and  $\overline{u_i u_j}$ , as the case may be.
8. Then solve the temperature equation.

These steps are repeated until convergence. A V-cycle multigrid algorithm is utilised with 10 iterations on the coarsest grid and 3 on intermediate grids. One or more iterations are carried out on the finest grid depending on the achieved smoothing rate. Restriction from fine to coarse grid is by averaging, and prolongation from coarse to fine grid is by trilinear interpolation. An ADI scheme is employed to solve the final set of algebraic equations for all variables at all grid levels. The underlying algorithm is the tri-diagonal matrix algorithm (TDMA) which is known to be recursive, and would thus not normally be vectorizable. However, by changing the data structure we can make all the internal loops of the ADI solver vectorizable on the Cray computers. Although we cannot remove the recursivity of the algorithm, the change in data structure ensures that all floating point operations are in vector form. Typical saving in total CPU time resulting from this is of the order of 50%.

The equations for turbulent quantities  $k$ ,  $\epsilon$  and  $\overline{u_i u_j}$  are solved only on the current finest grid during the iteration process. Corresponding operators on coarser grids are calculated using restricted values for these quantities. However, the solution process on any fine grid is started with variable values prolonged from the converged solution on the immediate coarser grid. This point is especially important for the Reynolds stresses.

## RESULTS AND DISCUSSION

### Computational Details

The test cases for the present work are derived from experimental studies of opposed jets discharging normally into a cross-stream by Atkinson et al [3]. Figure 1 shows the schematic diagram. Three cases are considered; two with a single pair of opposed jets and one with a row of five pairs. The computational details are presented in table 1, below.

Table 1 :Computational Details of Test Cases.

Case	R	S/D or W/D	Coarsest grid	Total Points on Finest Grid	CPU Time/ Work Units (Cray YMP mins)
1	1.8	12	12x10x22	876,744	39/82
2	1.0	12	12x10x22	876,744	34/71
3	1.8	4	8x10x22	534,600	27/94

In table 1, R represents the jet to crossflow velocity ratio, D is the jet diameter, W is the channel width in the single-pair jet study, and S is the jet-centreline pitch spacing in the multiple-pairs jet study. The channel height is 4D in all cases, so that there is a

symmetry plane at 2D. Cases 1 and 2 also have a symmetry plane passing through the centre of the jet and channel, whereas case 3 has a third symmetry plane through the mid-plane between jets. The inlet plane for the crossflow is located 4D upstream of the jet inlet and the outlet plane 14D downstream. We take advantage of the various symmetry planes to minimize the size of the computational domain. Figure 2 shows typical velocity vectors in the center plane computed with the RSM model on a 3-level grid. Details of the flow field are discernible in the exploded view (a). We can see the complex flow spiral in the wake, which shows how the crossstream passing between the jets is entrained into the jet. There is also a small reverse flow near the stagnation point in front of the jet. Further, for this velocity ratio, it is clear that the two opposing jets impinge upon each other along the symmetry plane, from about one diameter downstream of the exit pipes. The performance values in table 1 are for convergence to a normalised residual level of  $5 \times 10^{-4}$ . They represent the total computational work done on all grids for computations with the  $k - \epsilon$  turbulence model on a single processor. Computations with the Reynolds stress model typically require twice as many iterations. It now appears that the multigrid scheme should also be applied to the turbulence quantities  $k$ ,  $\epsilon$  and  $\overline{u_i u_j}$ . The computations presented in the paper are for 3- and 4-grid levels using the  $k - \epsilon$  turbulence model and 3-grid levels using RSM. 3-grid-level calculations take roughly 3–4 minutes.

## Grid Dependency

One of the main aims of the present study is to attempt to obtain grid-independent results through considerable grid refinement, so as to separate numerical errors from model errors. Figures 3–5 present the results of grid dependency tests. In Fig. 3, computed longitudinal velocity contours are compared along four axial planes for case 1. The computations on the right are on a grid which is exactly twice as fine as the one for the results on the left. We see that the flow patterns are exactly the same, but there are slight differences in peak values, especially in the near field. Figure 4, showing computed concentration/normalised temperature contours emphasizes these points. We also see steeper gradients near the edge of the jet for the finer grid computations, which is a result of reduced numerical diffusion. Figure 5 repeats these comparisons along two axial planes for case 3, which has the same velocity ratio as case 1 but for multiple pairs of jets. It is interesting to note that the results for these cases are similar, except for the higher velocity magnitudes and smaller jet spreading in case 3. These are of course due to the higher blockage factor in this case. Although the results cannot be claimed to be grid-independent the differences between them are small enough for us to estimate changes that could be expected from further grid refinement as compared with turbulence model changes. These results are for 3-level and 4-level grids. The next level of grid refinement will contain about 6.8 million points and should require about 256 megawords memory and 4 hours computational time. Although this is still within the capacity of the computer, the turnaround is expected to be very long.

## Comparison with Experiment

The present computations on a 3-level grid are compared with experimental results of Atkinson et al [3] in Figs. 6 and 7. The choice of grid is dictated by the little differences in predictions between 3- and 4-level grids shown in the preceding subsection, and the much greater expense of computations with RSM. Figure 6 presents the longitudinal velocity results for case 1 and fig. 7 those for case 2. For case 1, predictions with the  $k - \epsilon$  model at  $y^3/D = 4$  show the characteristic kidney shape. This is not evident in the measurements, and the RSM results show a much milder shape. It appears that the  $k - \epsilon$  model produces counter-rotating vortices that are too strong, leading to excessive distortion of the velocity contours. The Reynolds stresses act to reduce this motion and thus procure better agreement with the measurements. This trend is repeated in the results at  $y^3/D = 8$ . In general, the RSM model produces contour shapes that are much closer to the measurements than the  $k - \epsilon$  model. The magnitudes may not be exactly the same, but the trends are very encouraging, and the changes are certainly more significant than obtained through grid refinement. However, more work needs to be done to improve the RSM predictions. Concentration comparisons are not presented because these are not truly symmetrical in the experiments since only one jet was seeded in each case.

## CONCLUDING REMARKS

A multigrid procedure for calculating turbulent jets in crossflow has been presented. The procedure is applied with either a  $k - \epsilon$  turbulence model or a second-moment closure model. With the  $k - \epsilon$  model version, convergence can be obtained in less than 100 equivalent fine grid iterations on any grid. RSM version still needs some work to bring it to the same level of efficiency. Computations with the  $k - \epsilon$  model show slight changes with grid refinement, but the use of the RSM leads to much closer agreement of velocity contours with experimental data.

## ACKNOWLEDGEMENT

The computations were performed on the Cray YMP computer of the National Aerodynamics Simulation Program at NASA Ames Research Center, Moffet Field, California.

## REFERENCES

1. Y. Kamotani, and I. Greber, Experiments on a turbulent jet in crossflow, *AIAA J.* **10**, 1425-1429 (1972).
2. D. Crabb, D.F.G. Durao, and J.H. Whitelaw, A round jet normal to a crossflow, *ASME, J. Fluids Engg.* **103**, 142-153 (1981).

3. K.N. Atkinson, Z.A. Khan, and J.H. Whitelaw, Experimental investigation of opposed jets discharging normally into a cross-stream, *J. Fluid Mech.* **115**, 493–504 (1982).
4. J. Andreopoulos, and W. Rodi, An experimental investigation of jets in a crossflow *J. Fluid Mech.* **138**, 93–127 (1984).
5. J. Andreopoulos, On the structure of jets in a crossflow, *J. Fluid Mech.* **157**, 163–197 (1985).
6. S.A. Sherif, and R.H. Pletcher, Measurements of the flow and turbulence characteristics of round jets in crossflow, *ASME, J. Fluids Engg.* **111**, 165–171 (1989).
7. S.V. Patankar, D.K. Basu, and S.A. Alpay, Prediction of three dimensional velocity field of a deflected turbulent jet, *ASME, J. Fluids Engg.* **99**, 758–762 (1977).
8. W.P. Jones, and J.J. McGuirk, Computations of a round turbulent jet discharging into a confined crossflow, in: *Turbulent Shear Flows 2*, (Springer 1980) pp. 233–245.
9. A.O. Demuren, Numerical calculations of steady three-dimensional turbulent jets in cross flow, *Comp. Meth. App. Mech. Engg.* **37**, 309–328 (1983).
10. K.C. Karki, and H.C. Mongia, Recent developments in computational combustion dynamics, AIAA Paper No. AIAA-89-2808, (1989).
11. R.W. Claus, and S.P. Vanka, Multigrid calculations of a jet in crossflow, AIAA Paper No. AIAA-90-0444, (1990).
12. B.E. Launder, and D.B. Spalding, The numerical computation of turbulent flows, *Comp. Meth. App. Mech. Engg.* **3**, 269–289 (1974).
13. B.E. Launder, G.J. Reece, and W. Rodi, Progress in the development of a Reynolds stress turbulence closure. *J. Fluid Mech.* **68**, 537–566 (1975).
14. A. Brandt, Multi-level adaptive solutions to boundary-value problems, *Math. of Comp.* **31**, 330-390 (1977).
15. A.O. Demuren, Application of multi-grid methods for solving the Navier-Stokes equations, *Proc. Inst. Mech. Engrs.* **203**, 255–265 (1989).
16. S.P. Vanka, Block-implicit multi-grid solution of Navier-Stokes equations in primitive variables, *J. Comput. Phys.* **65**, 138–158 (1986).
17. M. Peric, A finite volume method for the prediction of three dimensional fluid flow in complex ducts, Ph.D. Thesis, (University of London, London 1985).

18. J.P. van Doormaal, and B.D. Raithby, Enhancements of the SIMPLE method for predicting incompressible fluid flows, *Numer. Heat Trans.* **7**, 147-163 (1984).

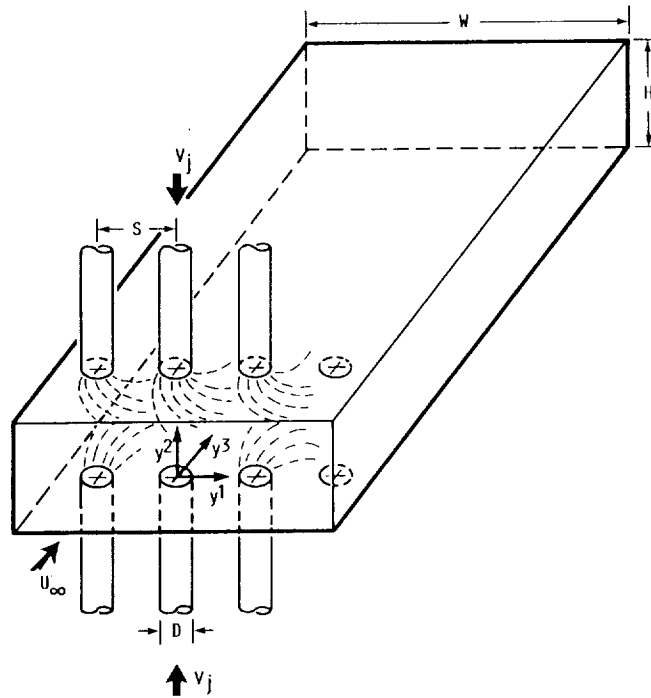
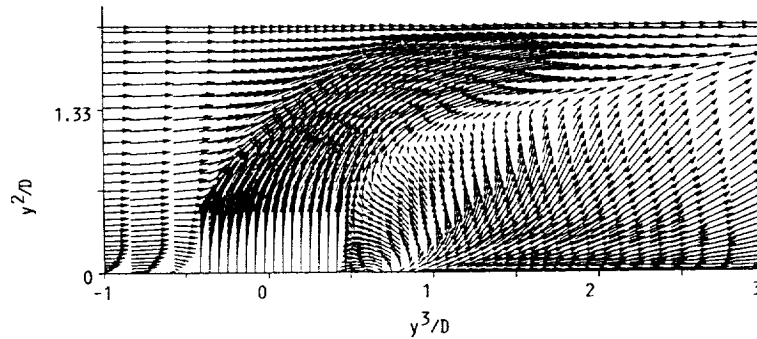
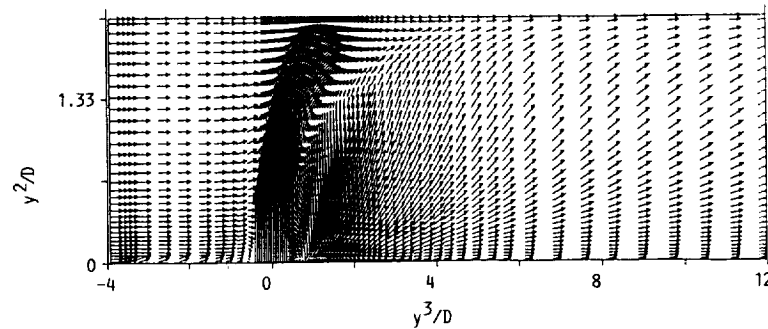


FIGURE 1. - MULTIPLE PAIRS OF OPPOSED JETS IN CROSSFLOW.



(a) NEAR FIELD.



(b) WHOLE FIELD.

FIGURE 2. - COMPUTED VELOCITY VECTORS IN CENTER-PLANE,  $R = 1.8$ ,  $W/D = 12$ .

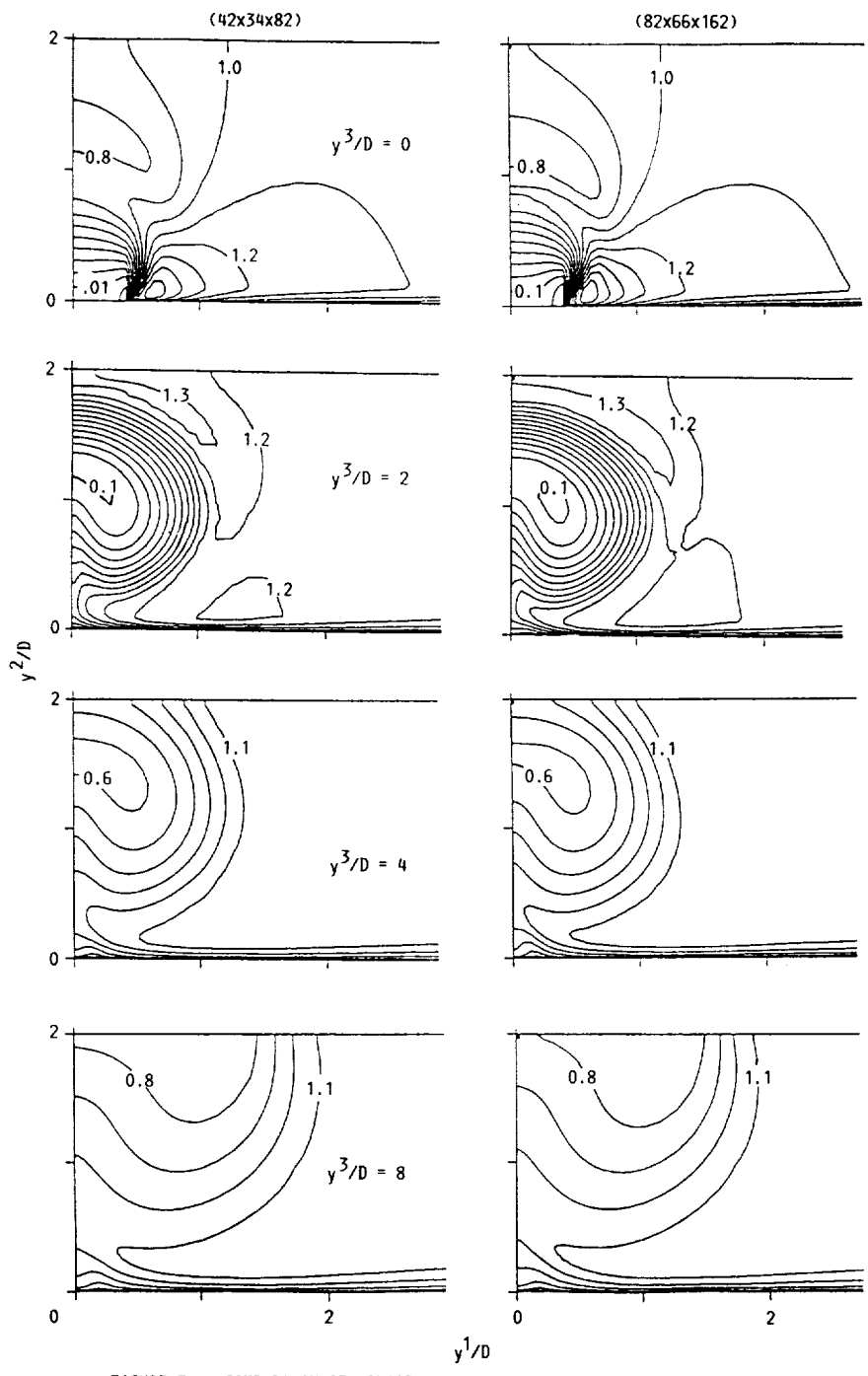


FIGURE 3. - COMPARISON OF LONGITUDINAL VELOCITY CONTOURS, R = 1.8, W/D = 12.

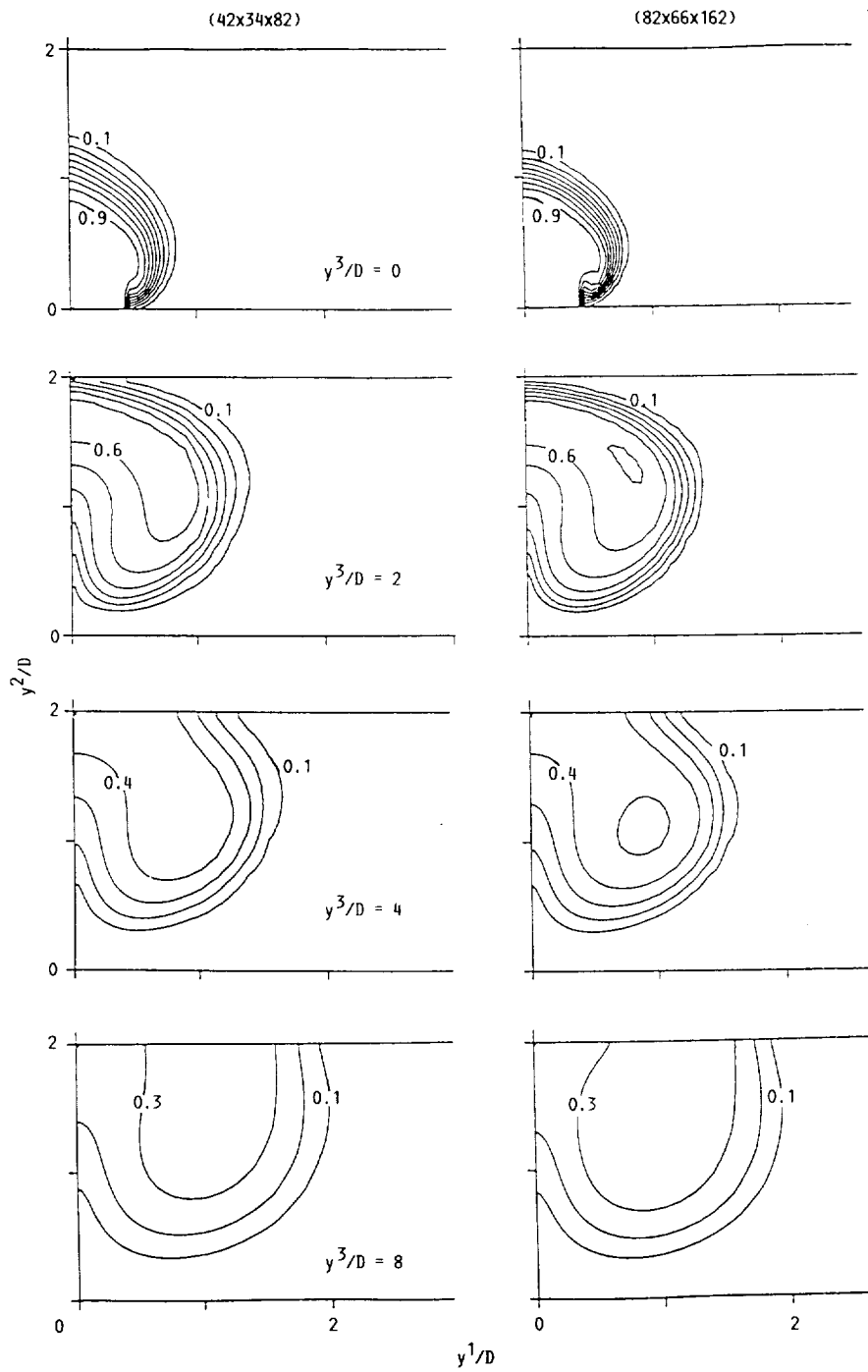


FIGURE 4. - COMPARISON OF CONCENTRATION CONTOURS,  $R = 1.8$ ,  $W/D = 12$ .

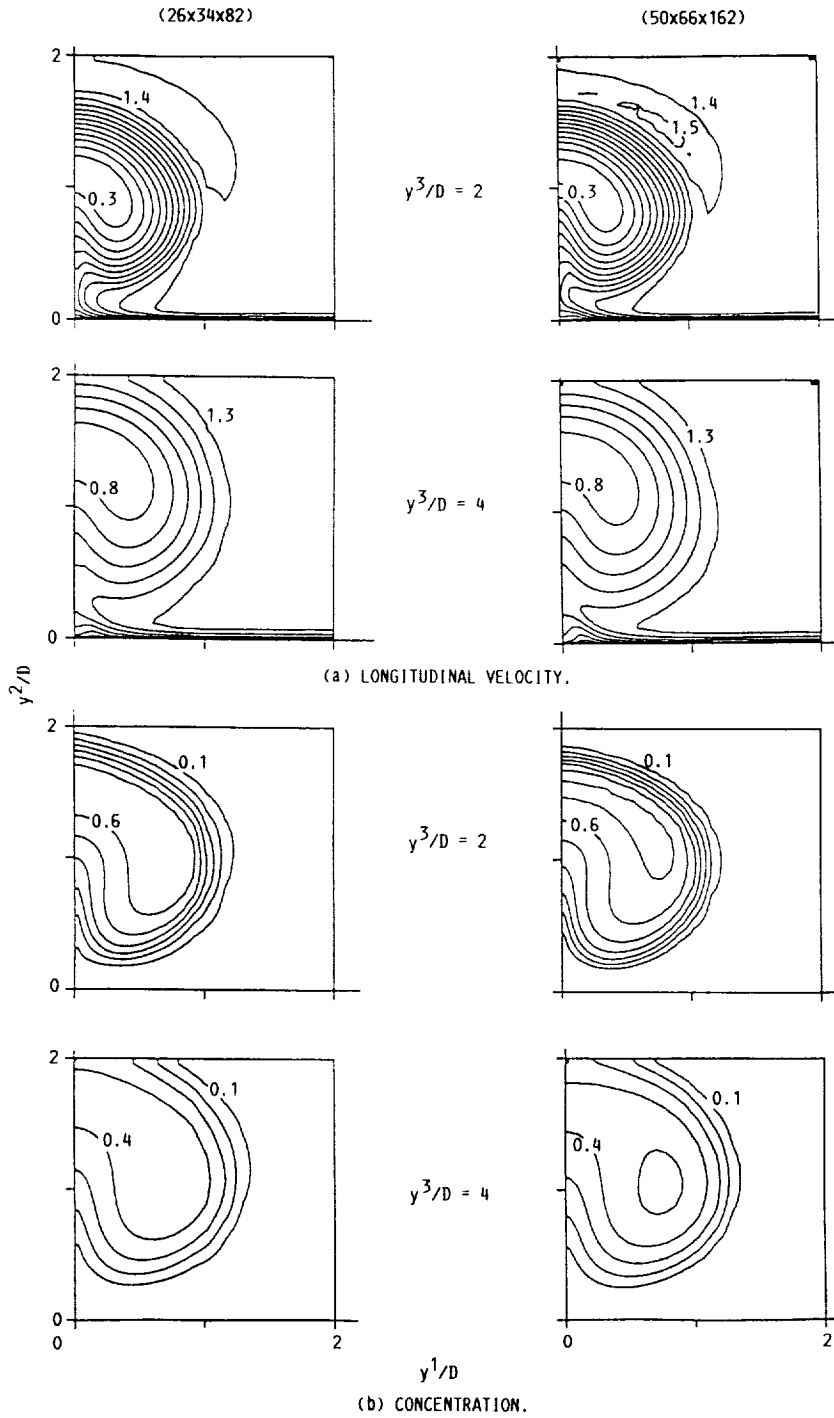


FIGURE 5. - COMPARISON OF PREDICTED CONTOURS.  $R = 1.8$ ,  $S/D = 4$ .

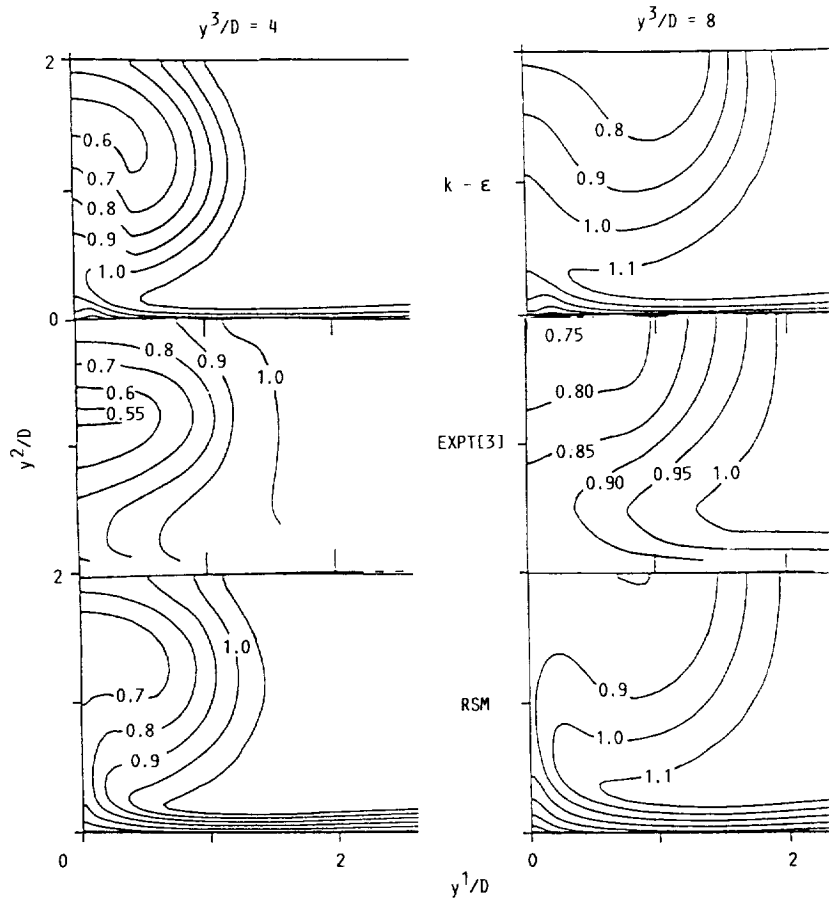


FIGURE 6. - COMPARISON OF LONGITUDINAL VELOCITY CONTOURS,  $R = 1.8$ ,  $W/D = 12$ .

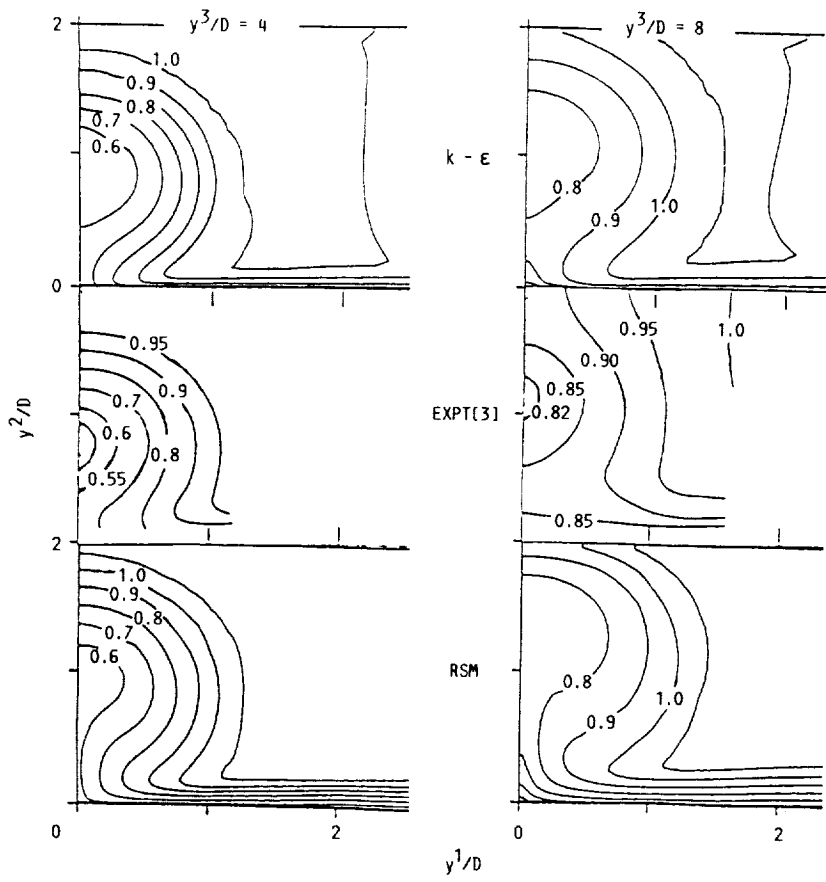


FIGURE 7. - COMPARISON OF LONGITUDINAL VELOCITY CONTOURS,  $R = 1.0$ ,  $W/D = 12$ .



National Aeronautics and  
Space Administration

## Report Documentation Page

1. Report No. NASA TM-103159 ICOMP-90-15		2. Government Accession No.		3. Recipient's Catalog No.	
4. Title and Subtitle Calculation of 3D Turbulent Jets in Crossflow With a Multigrid Method and a Second-Moment Closure Model				5. Report Date	
				6. Performing Organization Code	
7. Author(s) A.O. Demuren				8. Performing Organization Report No. E-5527	
				10. Work Unit No. 505-62-21	
9. Performing Organization Name and Address National Aeronautics and Space Administration Lewis Research Center Cleveland, Ohio 44135-3191				11. Contract or Grant No.	
				13. Type of Report and Period Covered Technical Memorandum	
12. Sponsoring Agency Name and Address National Aeronautics and Space Administration Washington, D.C. 20546-0001				14. Sponsoring Agency Code	
15. Supplementary Notes Prepared for the International Symposium on Engineering Turbulence Modelling and Measurements sponsored by the Assembly of World Conferences on Experimental Heat Transfer, Fluid Mechanics and Thermodynamics, Dubrovnik, Yugoslavia, September 24-28, 1990. A.O. Demuren, Institute for Computational Mechanics in Propulsion, Lewis Research Center, Cleveland, Ohio 44135 (work funded under Space Act Agreement C-99066-G). Louis A. Povinelli, Space Act Monitor.					
16. Abstract A multigrid method is presented for calculating turbulent jets in crossflow. Fairly rapid convergence is obtained with the $k-\epsilon$ turbulence model, but computations with a full Reynolds stress turbulence model (RSM) are not yet very efficient. Grid dependency tests show that there are slight differences between results obtained on the two finest grid levels. Computations using the RSM are significantly different from those with $k-\epsilon$ model and compare better to experimental data. Some work is still required to improve the efficiency of the computations with the RSM.					
17. Key Words (Suggested by Author(s)) Jets; Turbulence; Reynolds stress model; Second-moment closure; Multigrid; Computations; Finite-volume			18. Distribution Statement Unclassified - Unlimited Subject Category 34		
19. Security Classif. (of this report) Unclassified		20. Security Classif. (of this page) Unclassified		21. No. of pages 18	22. Price* A03

